Strain softening under bi-axial tension and compression

Autor(en): **Tanabe, Tada-aki / Wu, Zhishen**

Objekttyp: **Article**

Zeitschrift: **IABSE reports = Rapports AIPC = IVBH Berichte**

Band (Jahr): **62 (1991)**

PDF erstellt am: **12.07.2024**

Persistenter Link: https://doi.org/10.5169/seals-47693

Strain Softening under Bi-Axial Tension and Compression

Résistance du béton en cas de traction bi-axiale et de compression

Zweiaxiale Druck-Zug-Festigkeit gerissenen Betons

Tada-aki TANABE
Professor
Nagoya Univ.
Nagoya, Japan

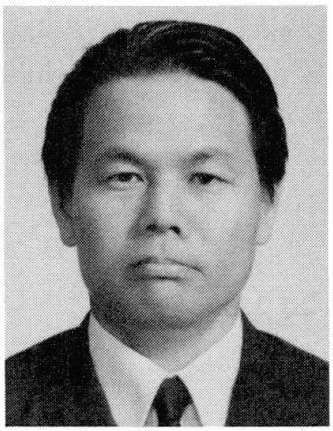

Since 1971, senior researcher at the Central Research Institute of Electric Power Industry. Since 1984, Professor in the Department of Civil Engineering, Nagoya University.

Zhishen WU
Res. Assoc.
Nagoya Univ.
Nagoya, Japan

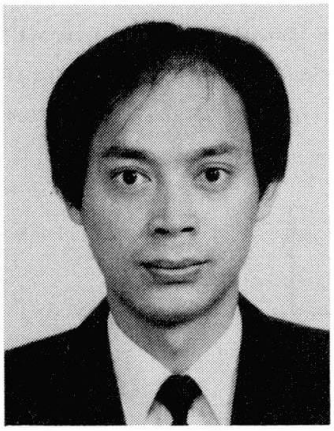

Obtained Dr. of Engineering degree at Nagoya University in 1990. Since then, research associate in the Department of Civil Engineering, Nagoya University.

SUMMARY

Strength criteria of concrete exhibiting strain softening have been derived based on a simple constitutive equation with much emphasis on the compressive strength reduction due to the tensile damage in the direction orthogonal to the compressive axis. The main experiments performed in Japan relating to the problem are described. Comparison of the theoretical reduction of the strength with the experimental data is made.

RÉSUMÉ

Les critères de résistance du béton dans le cadre du champ d'affaiblissement des contraintes ont dérivé d'une équation constitutive simple, où le point est mis sur l'abaissement de la résistance en compression. Celle-ci est due aux effets des efforts de traction dans la direction perpendiculaire à la direction de compression. Les expériences principalement effectuées au Japon à ce sujet sont présentées. Les données expérimentales obtenues sont comparées à la réduction théorique de la résistance.

ZUSAMMENFASSUNG

Es wurden einfache konstitutive Gleichungen für die Festigkeitskriterien von Beton gegeben, die besonders die Abnahme der Betondruckfesigkeit infolge Querzug und Rissbildung berücksichtigen. Die wichtigsten der in Japan durchgeführten Versuche zu diesem Problem werden vorgestellt, und es wird über die Vergleiche mit den theoretisch ermittelten Festigkeitsanwendungen berichtet.

1. INTRODUCTION

The research works related to the strength criteria or the failure surfaces in multi-axial stress states have advanced today to a substantial extent. However, most of these works are focused on the stress condition up until concrete reaches the maximum strength whether the stress may be in compression or in tension. Unlike the metallic material to which theoretical consideration for concrete constitutive equation owes to a great extent, the concrete material experiences strain softening after reaching its maximum point. The situation is same both for the compression failure and for tension failure.

It is well known that once concrete gets into the strain softening region, the stress strain relation becomes size dependent due to the strain localization. In the above situation, we naturally consider that the maximum strength will be different for the same amount of constraining stress to the transverse direction when one of the constraining stress is in elastic range while the other is in the softening range. The stress situation is shown in Fig.1.

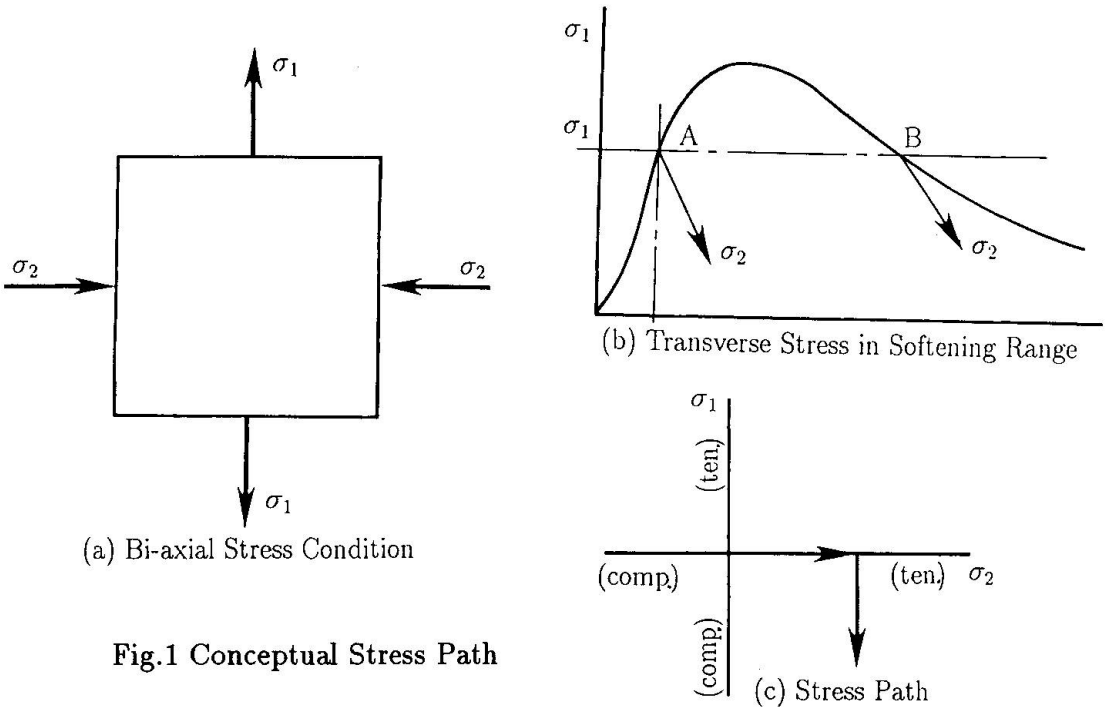

(a) Bi-axial Stress Condition

(b) Transverse Stress in Softening Range

(c) Stress Path

Fig.1 Conceptual Stress Path

The stress distribution of this kind is often encountered in shear problems of beams, walls and so on and it is generally recognized that the strength criteria for this situation is vitally important for the estimation of load bearing capacity. At present moment, the strength criteria for bi-axial tension and compression stress field in the softening zone is represented in terms of tensile strain in the transverse direction basing on the experimental results[1],[7],[8],[9],10]. However, it is desirable that the same characteristics may be expressed in more consistent way.

The current models proposed in CEB code[2] for the constitutive equation are essentially either homogeneous isotropic or orthotropic nonlinear elastic and they refer to the maximum stress point and do not refer to the strength reduction when the orthogonal stress is on the softening branch.

In other words, maintaining tensile stress σ_1 at point A in Fig.1-b and let require the maximum compressive strength of σ_2. The current constitutive equation can predict it rather accurately. However, σ_1 is maintained at point B in Fig.1-b and let require the maximum compressive strength of σ_2. It may not be altogether so well predictable.

With these reasons, they are not considered to fit for expressing above mentioned physical properties of concrete.

To cope with this problem, the adoption of work hardening and strain softening plasticity may be fitted[3]. However, the most rigorous work hardening and strain softening plasticity model which takes into account the strain localization may again have a difficulty for the adoption in this case since the tensile strain induced by the extension of buried-in reinforcement becomes appreciable amount, for example, 5000×10^{-6}, and the situation is different from simple tension. It is obvious that the strain softening and the strain localization in this case have been so much dispersed. With these reasons, the fracture energy based plasticity formulation is not applicable when we try to treat it in an average way.

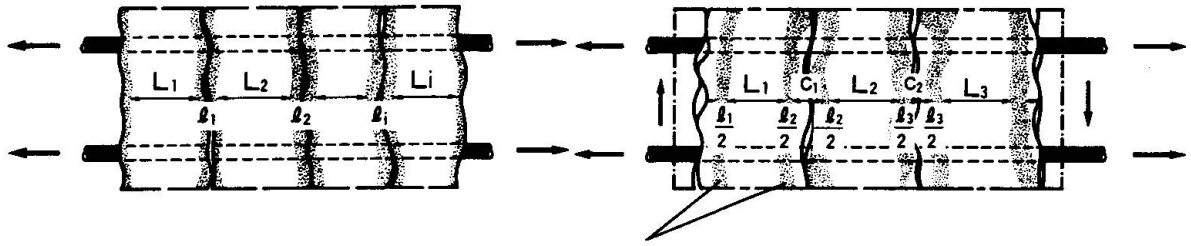

(a) Pure Tension (b) Tension and Shear

Fig.2 Reinforcement Induced Strain Fields of Concrete

Suppose,we have a uniaxial tension member as shown in Fig.2-a. It is clear that we have several zones which are in strain softening fields and the same number of zones which are in elastic fields. The average tensile strain there, then, are written as

$$\varepsilon_n = \frac{1}{\ell}\left[\sum_i \int_0^{Li} \varepsilon_e dx + \sum_j \int_0^{\ell j} \varepsilon_p dx + \sum_k w_k\right] \tag{1}$$

where ε_e and ε_p denote tensile strains in elastic regions and in softening regions respectively. The term w_k denotes kth crack width.

In the practical purpose of expressing concrete strength in the softening region,the averaged strain of the first and second term of Eq.(1) are important except for those cases when the detailed stress analysis which distinguishes the tensile strain in the softening zone and the strain in other zones are carried out.

When shear transfer occurs at a crack, the strain softening region is forced back to the central portion by the compression zone which has been induced by shear friction and the elastic tensile zone may be occupying the central portion. More detailed discussion will be found in the reference[4]. In consequence, the tensile strain distribution is considered to be more uniform, localization being less effective due to the existence of reinforcement. In this sense, we may be

able to adopt the simpler work hardening and softening plasticity model.

In this report, we will try to express the strength criteria in these situation by hardening and softening plasticity so that the simple and more consistent strain and stress relation may become possible without considering the strain localization.

2. Theoretical Consideration

2.1 Plastic Strain Formulation

The present formulation follows essentially the basic concept of the classical theory of hardening plasticity for the sake of its simplicity. The position of the subsequent failure surface is assumed to change its size continuously depending on the damage accumulated in the concrete material, i,e. the failure surface is a function of the plastic work $\omega(W^p)$.

$$f = f(\sigma_{ij}, \omega(W^p)) = 0 \tag{2}$$

where W^p denotes the plastic work accumulated after the initial failure, and σ_{ij} denotes the Cauchy's stress tensor. An independent function, i.e. plastic potential function g is defined as

$$g = g(\sigma_{ij}, \omega(W^p)) = 0 \tag{3}$$

Generally, the application of the classical plasticity theory implies that the total strain rate is composed of the elastic and the plastic part

$$\dot{\varepsilon}_{kl} = \dot{\varepsilon}^e_{kl} + \dot{\varepsilon}^p_{kl} \tag{4}$$

The plastic strain rate tensor then, is assumed to be from the plastic potential g as

$$\dot{\varepsilon}^p_{kl} = \lambda \frac{\partial g}{\partial \sigma_{kl}} \tag{5}$$

while the elastic strain rate tensor ε^e_{kl} is assumed to be related to the stress rate tensor via the elasticity tensor D^e_{ijkl}

$$\dot{\sigma}_{ij} = D^e_{ijkl}\dot{\varepsilon}^e_{kl} \tag{6}$$

where λ is a non-negative multiplier which can be determined from the consistency condition during loading.

Consequently, the consistency condition $\dot{f} = 0$ can be expressed as

$$\dot{f} = \frac{\partial f}{\partial \sigma_{ij}}\dot{\sigma}_{ij} + \frac{\partial f}{\partial W^p}\dot{W}^p \tag{7}$$

where $\dot{W}^p$ can be written as

$$\dot{W}^p = \sigma_{ij}\dot{\varepsilon}^p_{ij} \tag{8}$$

Substituting Eqs.(4),(5),(6) and (8) into Eq.(7) and solving for λ , yields

$$\lambda = \frac{\frac{\partial f}{\partial \sigma_{ij}} D^e_{ijkl} \dot{\varepsilon}_{kl}}{\frac{\partial f}{\partial \sigma_{mn}} D^e_{mnpq} \frac{\partial g}{\partial \sigma_{pq}} + h} \tag{9}$$

with a definition of

$$h = -\frac{\partial f}{\partial W^p} \sigma_{ij} \frac{\partial g}{\partial \sigma_{ij}} \tag{10}$$

Note that $\partial f/\partial W^p$ in Eq.(7) and Eq.(10) will be a negative value for the hardening behavior and a positive value for the softening behavior. As in the classical theory of plasticity, the subsequent yield surface can be expressed with multiparameter $\xi_1, \xi_2, \ldots, \xi_i, \ldots$

$$f(\sigma_{ij}, \xi_1(\omega), \xi_2(\omega), \cdots, \xi_i(\omega), \cdots) = 0 \tag{11}$$

Here, a series of these parameters are assumed to be unique functions of the damage parameter ω and defined to characterize the shape and size of the yield surfaces. The initial loading surface is assumed to coincide with the elastic limit surface. The subsequent yield surface expands with the increase of inelastic strains in hardening. After a state of stress reaches the ultimate condition named as the initial failure surface, the subsequent yield surface will begin to reduce its size continuously until it reaches the final failure state named as the final failure surface.

The function $\partial f/\partial W_p$ can be elaborated, then as

$$\frac{\partial f}{\partial W^p} = \left(\frac{\partial f}{\partial \xi_1}\frac{\partial \xi_1}{\partial \omega} + \frac{\partial f}{\partial \xi_2}\frac{\partial \xi_2}{\partial \omega} + \cdots + \frac{\partial f}{\partial \xi_i}\frac{\partial \xi_i}{\partial \omega} + \cdots\right)\frac{\partial \omega}{\partial W^p} \tag{12}$$

2.2 Definition of the Damage Parameter

Before discussing the damage parameter, let recall the concept of effective stress σ_e and effective plastic strain ε_p[5]. An effective plastic strain rate $\dot{\varepsilon}_p$ is defined in relation with the plastic work rate $\dot{W}_p$ as

$$\dot{W}^p = \sigma_{ij}\dot{\varepsilon}^p_{ij} = \sigma_e \dot{\varepsilon}_p \qquad (\dot{\varepsilon}_p > 0) \tag{13}$$

It is easily found that the single effective stress- effective plastic strain curve should preferably be reduced to a uniaxial stress-strain curve for a uniaxial stress test.

The damage parameter defines the damage of the material accumulated due to the progressive growth of the micro cracks etc., which is defined for convenience, in the form of

$$\omega = \frac{\beta}{\sigma_e \varepsilon_0} \int dW^p \tag{14}$$

where, β is a material constant, and

$$\varepsilon_0 = \frac{f'_c}{E_c} \tag{15}$$

Here, E_c denotes the modules of elasticity of concrete, and f'_c is the uniaxial compressive strength. Substituting Eq.(12) into Eq.(13), we have

$$\omega = \beta \int d\varepsilon_p/\varepsilon_0 \tag{16}$$

2.3 Application of Drucker-Prager Type Failure Surface

Although more sophisticated criteria may be preferable for simplicity, the following Drucker-Prager type yield criterion is employed for its simplicity.

$$f = \sqrt{J_2} + \alpha_f I_1 - k_f = 0 \tag{17}$$

Besides, a similar expression for the plastic potential function is assumed as

$$g = \sqrt{J_2} + \alpha_g I_1 - k_g = 0 \tag{18}$$

where $I_1 = \sigma_{kk}$ and $J_2 = \frac{1}{2} s_{ij} s_{ij}$ are the first invariant of stress tensor σ_{ij} , and the second invariant of deviatoric stress tensor s_{ij}, respectively, and α_f ,k_f, α_g and k_g are material constants.

Since it is known that the Mohr-Coulomb criterion is simple with constants of a clear physical meaning which are related to the uniaxial strength straightforwardly, the Drucker-Prager cone is matched with it such that two surfaces are made to agree along the compressive meridian. In this case, the two sets of material constant are related by

$$\alpha_f = \frac{2sin\phi^*}{\sqrt{3}(3 - sin\phi^*)}, k_f = \frac{6c^* cos\phi^*}{\sqrt{3}(3 - sin\phi^*)} \tag{19}$$

where ϕ^* and c^* are two strength parameters in the Mohr-Coulomb criterion, namely the so-called mobilized friction angle and mobilized cohesion [6], and the notation '*' is introduced to indicate that ϕ^* and c^* are not constant but depend on the plastic strain history through the damage parameter ω. In spite of the paucity of experimental data to support the definition of the damage parameter ω , we are able to say something about the dependence of ϕ^* and c^* on ω . The value of ϕ^* generally should be an ascending function of ω, while c^* may be expected to be a descending function of ω. Possible relations for the hardening and softening model are suggested as follows

$$c^* = cexp[-(m\omega)^2] \tag{20}$$

$$\begin{cases} \phi^* = \phi_0 + (\phi - \phi_0)\sqrt{2\omega - \omega^2} & \omega \leq 1 \\ \phi^* = \phi & \omega > 1 \end{cases} \tag{21}$$

where, m is a material parameter. The notations c and ϕ denote the cohesion and the internal-friction angle of the concrete respectively. All of these relations are shown in Fig.3.

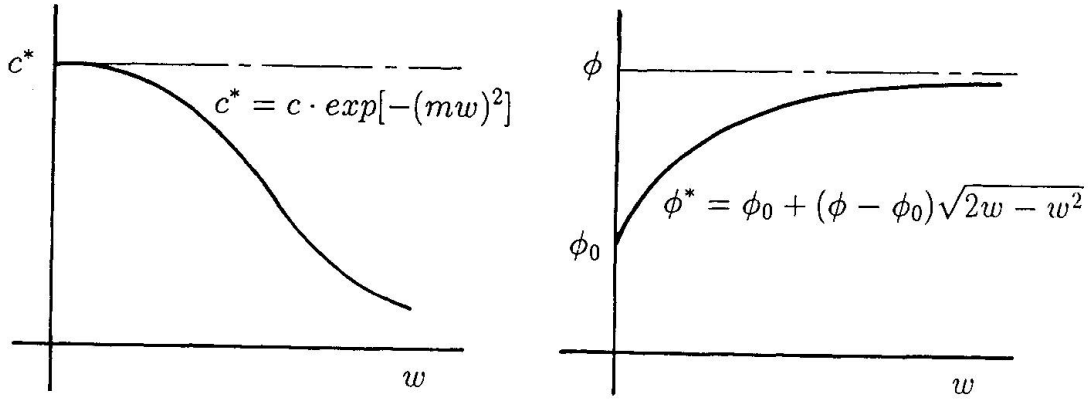

Fig.3 Possible Relations of $c^* - w$ and $\phi^* - w$

Similarly, we defined

$$\alpha_g = \frac{2sin\psi^*}{\sqrt{3}(3 - sin\psi^*)}, k_g = \frac{6c^*cos\psi^*}{\sqrt{3}(3 - sin\psi^*)} \tag{22}$$

with a defined mobilized dilatancy angle ψ^* . It is noted that for $\psi^* = \phi^*$, we have $f = g$ and the classical associated flow rule is recovered.

2.4 Flow Rule

The associated flow rule is applied predominantly for practical reasons, since no experiments have been conducted on subsequent loading surfaces for concrete materials. For associated flow rule, it is interesting to note the plastic work rate is

$$\dot{W}^p = \sigma_{ij}\dot{\varepsilon}^p_{ij} = \lambda\sigma_{ij}\frac{\partial f}{\partial \sigma_{ij}} = \lambda\sigma_{ij}\frac{\partial F}{\partial \sigma_{ij}} = \lambda nF \tag{23}$$

when $F(F = f + k)$ is homogeneous of degree n in the stresses, as it is for many cases in plasticity theories. The scalar function λ can be obtained by squaring each of the terms in Eq.(5) and adding as

$$\dot{\varepsilon}^p_{ij}\dot{\varepsilon}^p_{ij} = \lambda^2\frac{\partial F}{\partial \sigma_{ij}}\frac{\partial F}{\partial \sigma_{ij}} \tag{24}$$

Taking the square root of both sides and substituting λ into Eq.(23) shows that $\dot{\varepsilon}_p$ must be a function of F and $\sqrt{\dot{\varepsilon}^p_{ij}\dot{\varepsilon}^p_{ij}}$

$$\dot{\varepsilon}_p = \frac{\dot{W}^p}{\sigma_e} = \frac{\sqrt{\dot{\varepsilon}^p_{ij}\dot{\varepsilon}^p_{ij}}nF}{\sqrt{(\frac{\partial F}{\partial \sigma_{mn}})(\frac{\partial F}{\partial \sigma_{mn}})}\sigma_e} \tag{25}$$

where we have used the definition of plastic work(Eq.(13)) for defining the effective plastic strain ε_p. For the Drucker-Prager failure surface, the effective stress for the failure function can be obtained by substituting the uniaxial compressive stress condition into the function

$$\sigma_e = \frac{\sqrt{J_2} + \alpha_f I_1}{(\sqrt{1/3} - \alpha_f)} = \frac{k_f}{(\sqrt{1/3} - \alpha_f)} \tag{26}$$

By substituting Eq.(26) into Eq.(25), Eq.(25) can be reduced to

$$\dot{\varepsilon}_p = \frac{(-\alpha_f + 1/\sqrt{3})}{\sqrt{3\alpha_f^2 + 1/2}}\sqrt{\dot{\varepsilon}^p_{ij}\dot{\varepsilon}^p_{ij}} \tag{27}$$

Depending on the preceding discussion, $\partial f/\partial W^p$ in Eq.(12) for the Drucker-Prager criterion can be rewritten as

$$\frac{\partial f}{\partial W^p} = (\frac{\partial f}{\partial \alpha_f}\frac{\partial \alpha_f}{\partial \omega} + \frac{\partial f}{\partial k_f}\frac{\partial k_f}{\partial \omega})\frac{\partial \omega}{\partial W_p} = (I_1\frac{\partial \alpha_f}{\partial \omega} - \frac{\partial k_f}{\partial \omega})\frac{\partial \omega}{\partial W^p} \tag{28}$$

Here,

$$\frac{\partial \alpha_f}{\partial \omega} = \frac{2\sqrt{3}cos\phi^*}{(3-sin\phi^*)^2}\frac{\partial \phi^*}{\partial \omega} \tag{29}$$

$$\frac{\partial k_f}{\partial \omega} = \frac{6c^*(1-3sin\phi^*)}{\sqrt{3}(3-sin\phi^*)^2}\frac{\partial \phi^*}{\partial \omega} - \frac{12cm^2\omega}{\sqrt{3}(3-sin\phi^*)}e^{-(m\omega)^2}cos\phi^* \tag{30}$$

and

$$\frac{\partial \phi^*}{\partial \omega} = \begin{cases} \frac{(1-\omega)(\phi-\phi_0)}{\sqrt{2\omega-\omega^2}} & \omega \leq 1 \\ 0 & \omega > 1 \end{cases} \tag{31}$$

Moreover,

$$\frac{\partial \omega}{\partial W^p} = \frac{\beta}{\varepsilon_0 \sigma_e} \tag{32}$$

2.5 The c and ϕ Factors Affected by The Damage Parameter ω

The relation between the damage parameter ω and the c, ϕ will not be set in a unique way. At present study,however, we adopted the above mentioned equation. In these formulations, ω and c, ϕ change as shown in Fig.3 depending on the value of ω. The movement of failure surface with the increase of damage ω is shown in Fig.4 conceptually.

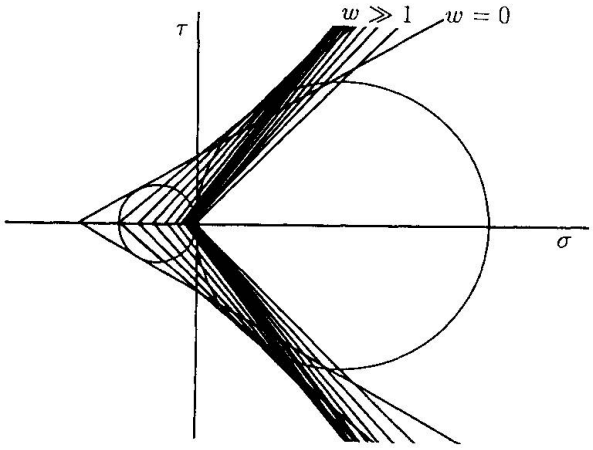

Fig.4 The Movement of Failure Surface

Looking at the figure, it may be understood that the maximum uniaxial compressive strength will be given by the circle which will make tangential contact with one of the lines with the maximum radii.

It is possible to select other relations between the damage parameter and failure parameter of c, and ϕ. As an example, several of the experimental data are compared in Fig.5 with the above mentioned criteria and reasonable agreement will be seen in the comparison for different loading paths.

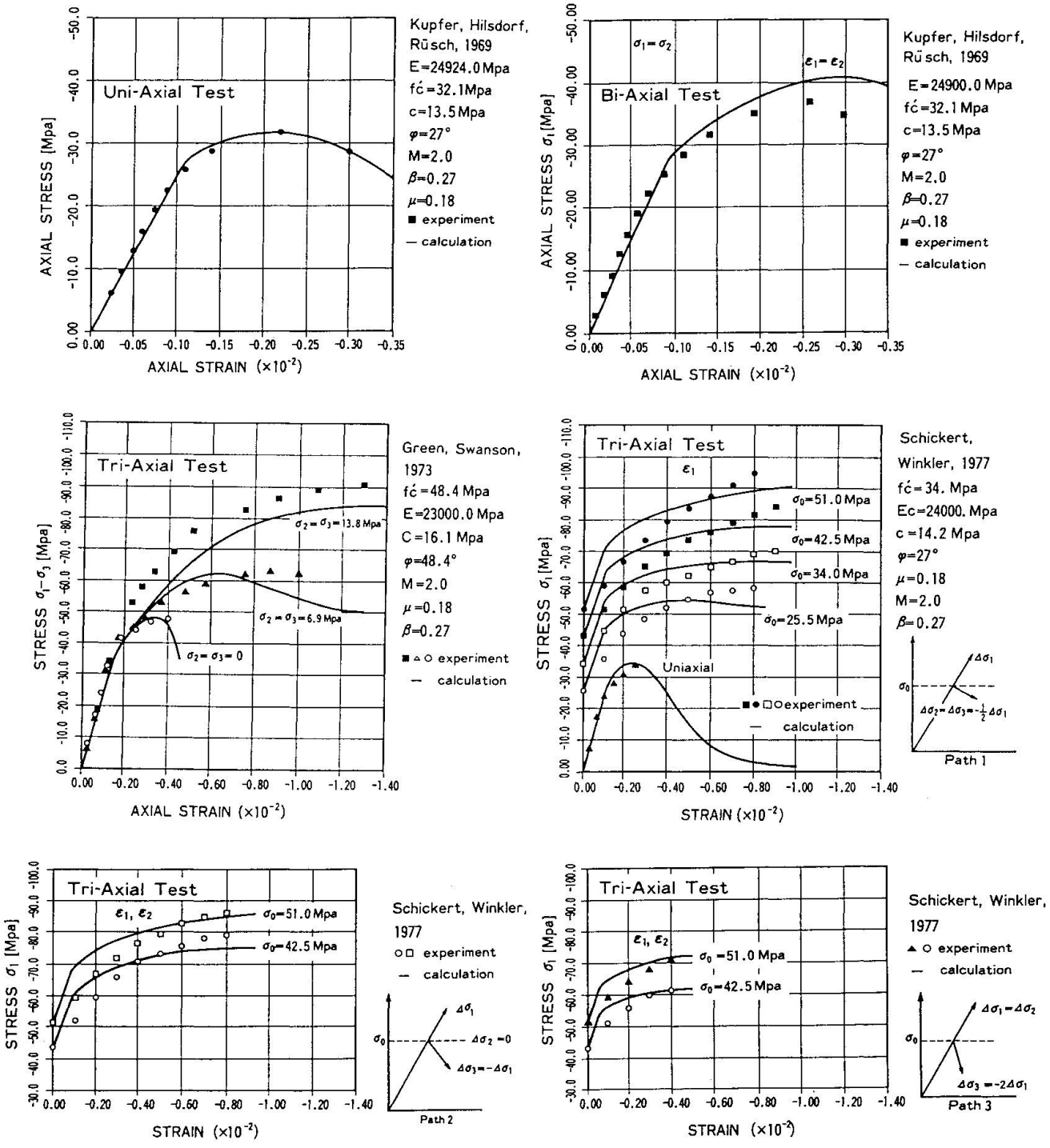

Fig.5 Comparison of Calculation and Experiments of Various Stress Paths

3. Experimental Results for The Bi-axial Tension and Compression

3.1 Vecchio and Collins' Test

In the beginning, it should be mentioned that those test results which are treated in this section are by no means bi-axial tension and compression test in its true sense. However,as mentioned in previous section, we try to utilize the results in the average sense and apply the theoretical criteria for those experimental results. At present moment, we have several experimental results for the stress field where one principal stress is in tension of the strain softening zone and the other principal stress is in compression, since the appearance of Vecchio and Collins reports[1] on the load carrying capacity of the panels subjected to in-plane shearing load. In that argument, treating the concrete element between the parallel cracks in uniformly stressed condition, he proposed the compressive strength reduction according to the amount of tensile strain to the transverse direction. The strength reduction was found to be the vital material characteristic which should be clarified to the detail since the strength of the member in shear depends upon the strength to such an extent. His proposal of strength reduction was as such that

$$\lambda = \frac{1}{0.80 + 0.34\left(\frac{\varepsilon_{1u}}{\varepsilon_0}\right)} \tag{33}$$

where ε_0 denotes the uniaxial compressive strain corresponding to the uniaxial compression strength of cylinder and ε_{1u} denotes the transverse tensile strain occurring.

3.2 Maekawa and Okamura's Test

In Japan, several experiments relating on this problem have been performed. Maekawa and Okamura[7] performed bi-axial tension and compression test using the cylindrical specimen. Inside the cylinder, water pressure was generated and ring tension was induced. The compressive strength,then obtained by the axial compression. They proposed the compressive strength reduction in the following form,

$$\begin{aligned} \lambda &= 1.0 && (\varepsilon_1 < \varepsilon_a) \\ &= 1.0 - 0.4\tfrac{\varepsilon_1 - \varepsilon_a}{\varepsilon_b - \varepsilon_a} && (\varepsilon_a \le \varepsilon_1 \le \varepsilon_b) \\ &= 0.6 && (\varepsilon_0 < \varepsilon_1) \\ \varepsilon_a &= 0.0012 \\ \varepsilon_b &= 0.0044 \end{aligned} \tag{34}$$

where ε_1 is the transverse tensile strain.

3.3 Sumi and Kawamata's Test

Sumi and Kawamata[8] has performed the most comprehensive experiment on the stress strain relation of cracked reinforced concrete panel elements using the specimens and the loading apparatus shown in Fig.6. For the equal reinforcement ratio in two orthogonal directions, they obtained the relation in the form of Eq.(35). They could measure the strain directly which corresponds to the first and second term of the Eq.(1) and the stress was calculated from the equivalence of the force to two directions.

$$\frac{\sigma_1}{f'_c} = f(\varepsilon_1)\left(1.5 + \frac{\varepsilon_{cr}}{\varepsilon_0}\right) - \left(\frac{\varepsilon_1}{\varepsilon_0}\right)^2 \tag{35}$$

where f'_c: uniaxial compressive strength of cylinder, ε_0: compressive strain which corresponds to f'_c, σ_1: compressive stress of cracked element, ε_1: compressive strain which corresponds to σ_1, and ε_{cr}: compressive strain of cracked element when transverse cracking initiated.

For the panels of unequal reinforcement ratio, the shear stress is transferred across the crack surfaces which add another factor for the stress strain relation in the cracked concrete element. With the similar method, they calculated the stress and strain. Finally, they proposed for this case the following equation.

$$\frac{\sigma_1}{f'_c} = \lambda f(\varepsilon_1)$$

$$\lambda = \frac{\left(4\frac{\sigma_2}{f'_c} + \frac{\sigma 1-max}{f'_c}\right)}{\left(\frac{\sigma_{1-max}}{f'_c}\right)} \tag{36}$$

where σ_2 denotes the stress in transverse direction while other notations appeared in Eq.(35).

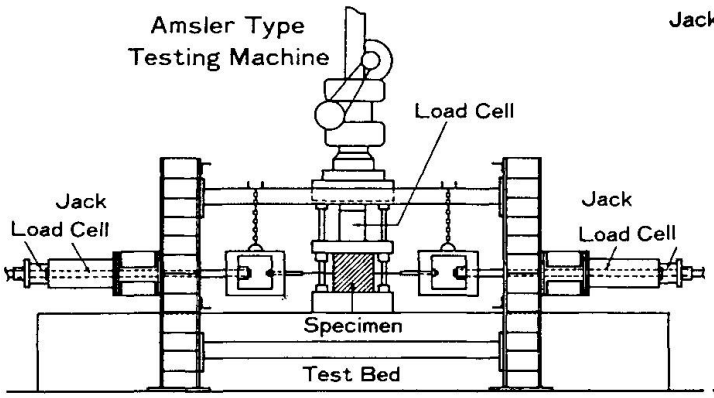

Fig.7 Shirai's Testing Method

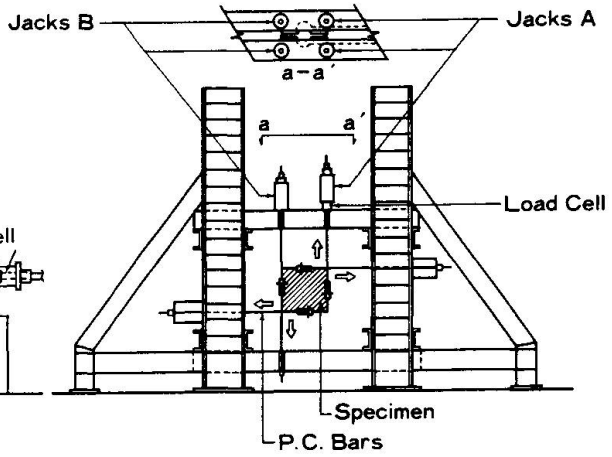

Fig.6 Sumi's Testing Method

The equation, however, gives higher strength when the orthogonal stress is in higher tension. In other word, this is contrary to the tendency reported in the past that the strain get larger, the stress is more reduced in the softening range and the strength in compression get smaller.

3.4 Shirai's Test

Shirai[9] performed experiment with the small specimen shown in Fig.7 and proposed the following equation.

$$\lambda_1 = -\left(\frac{0.31}{pi}\right) tan^{-1}\left[4820\varepsilon_1 - 11.82\right] + 0.84$$

$$\lambda_2 = -5.9\frac{f_{c1}}{f'_c} + 1.0$$

$$\lambda = \lambda_1 \cdot \lambda_2 \tag{37}$$

where f'_{c1} denotes the tensile stress working to the orthogonal direction.

3.5 Noguchi's Test

Noguchi[10] performed similar experiment and concluded the strength reduction in the form of

$$\lambda = \frac{1}{0.27 + 0.96(\frac{\varepsilon_{1u}}{\varepsilon_0})^{0.167}} \tag{38}$$

where ε_{1u} denotes average tensile strain to the transverse direction when the element fails in compression and ε_0 denotes the compressive strain of cylinder which corresponds to the uniaxial compressive strength of cylinder.

3.6 Comparison of the Theoretical Calculation and Results

All the experiments mentioned in the previous section showed that the failure surface shrink with the increase of tensile strain as shown in the Fig.8. It is also expected that the same strength reduction may occur in the softening compression and compression range though there have not been reported any experimental results so far.

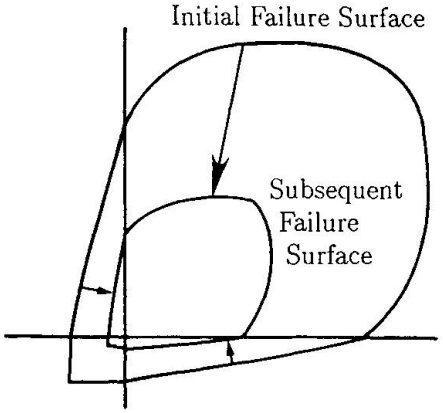

Fig.8 Shrinking Failure Surface

For those experimental results, the plasticity model mentioned in the previous section is applied. The concrete with uniaxial compression strength of 30 Mpa. has been loaded in various loading path. The one which has been the main topics of the present study is to load in uniaxial tension over the maximum point then stop the loading at some point in the softening range and starts to load it in compression to orthogonal direction keeping the damage which has been accumulated in previous loading path.

In this study, the accumulated damage ω was continued though the loading direction has changed 90 degrees and the maximum compression strength was calculated. Strength reduction which depend on the ratio are obtained and shown in Fig.9 in comparison with the experimental results which is the reproduction of Shirai's experimental results, however, being recalculated so that the strain of the coordinate be the 1st and second term of Eq.(1).

It may be seen that the reduction is in accordance with those proposed in the strain range

of 0 to 5000 $\times$ 10^{-6}. This is the numerical simulation for the purpose to show that the simple model proposed enable to trace the post peak strength reduction in reasonable way. However,it is true yet that we need more detailed study to relate modeling parameter with the actual condition of cracked reinforced concrete.

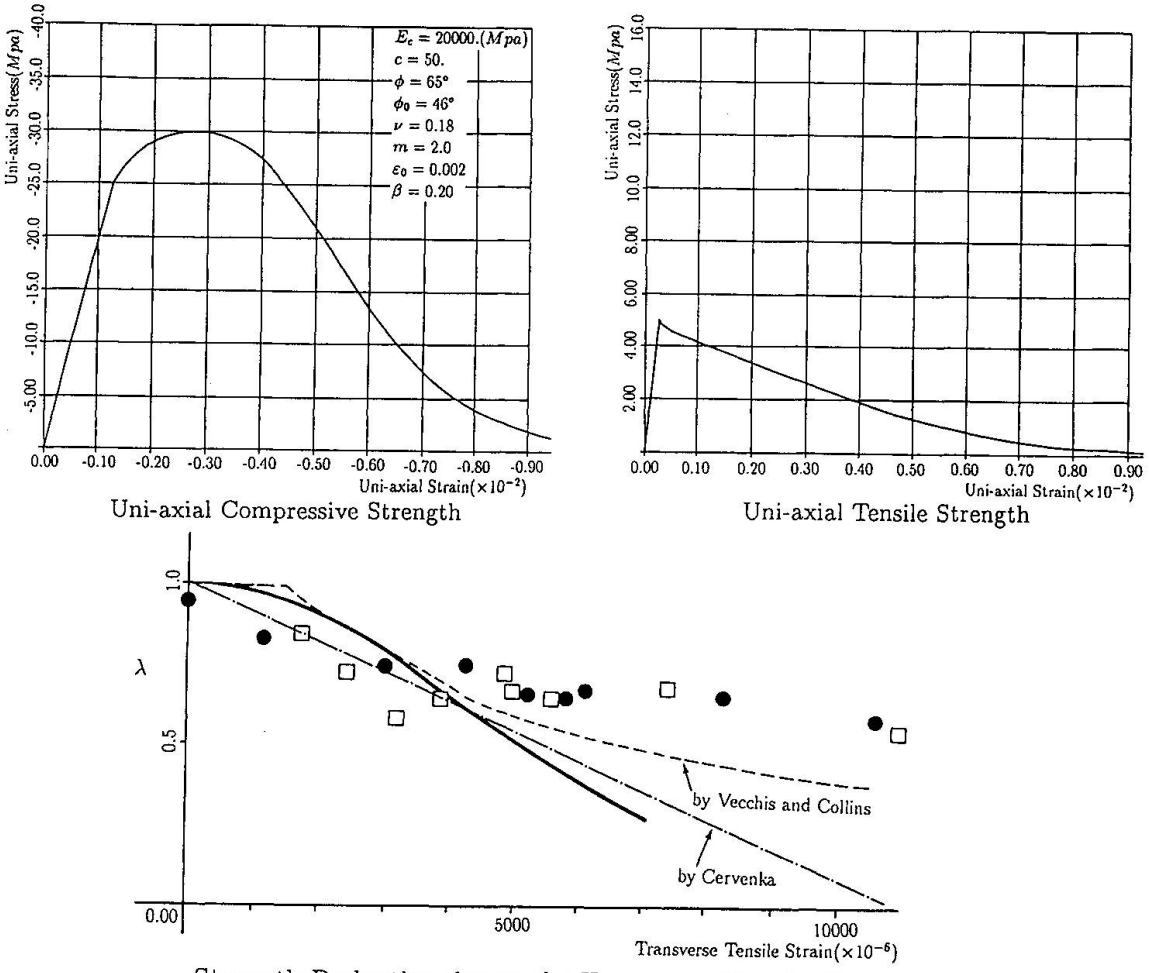

Fig.9 Strength Reduction Calculated

4. Conclusion

In the limit state design of reinforced concrete, it is paramount requisite to make a good estimate of the ultimate load carrying capacity of structures. For commonly met structures like beams, slabs and walls, the concrete behavior in bi-axial tension and compression stress field has a substantial effect for their load carrying capacity especially when shear effect is predominant. The compressive strength reduction in one of the principal direction when the orthogonal tension is occurring to the other principal direction has been the phenomena that draw concrete engineer's attention. As the tensile strain is mainly in the large strain range of softening, which is composed of elastic strain and localizing strain, the stress field is neither easily experimentally measurable nor analytically obtainable. However, we definitely need more comprehensive, consistent and reliable knowledge in that area. The consistent mathematical representation of the phenomena has been made in this study and some numerical examples were shown. However, it is much desired that the more experimental results be accumulated

not only in tension compression area but compression and compression area. Finally, thanks are due to the graduate student K. Taniyama and Ge Hanbin who has carried out the numerical calculation and especially to H. Nagashima for preparing the manuscript in this study.

References

[1] Vecchio,F., and Collins,M.P., The Response of Reinforced Concrete to In-plane Shear and Normal Stresses, University of Toronto, Publication No.82-03 March 1982.

[2] CEB-FIP Model Code 1990 First Draft, CEB Bulletin, No.195, March 1990.

[3] Pramono,E., and Willam,K., Fracture Energy-Based Plasticity Formulation of Plain Concrete, ASCE, EM 1988.

[4] Tanabe,T., and Yoshikawa,H., Constitutive Equation of a Cracked Reinforced Concrete Panel, IABSE Colloquim on Computational Mechanics of Concrete Structures, Delft, pp.17-34.

[5] Chen,W.F., Plasticity in Reinforced Concrete, Mc Grawttill, New York.

[6] Vermeer,P.A., and de Borst,R., Non-Associated Plasticity for Soils and Rock, Heron, 29, No.3, pp1-64.

[7] Okamura,H., and Maekawa,K., Nonlinear Analysis of Reinforced Concrete, Proc. of JSCE, No.360,Aug.1987,pp.1-10.

[8] Sumi,K.,and Kawamata,S., Properties of Cracked Concrete in the RC WallS subjected to In-Plane Shear, Concrete Journal, Vol.27, No.10, JCI, pp.97-107.

[9] Shirai,N..and Noguchi,H., Compressive Deterioration of Cracked Concrete, ASCE Structures Congress and Pacific Rim Engineering, San Francisco, May 1989.

[10] Hamada,S., and Noguchi,H., Basic Experiments the Degradation of Cracked Concrete under Bi-axial Compression and Tension, The Annual Report of the AIJ, Structures, Oct.1988, pp.397-398.